Angular Distributions of Scattered Neutrons*

A. LANGSDORF, JR., R. O. LANE, AND J. E. MONAHAN
Argonne National Laboratory, Lemont, Illinois

(Received March 11, 1957)

The angular distribution of neutrons scattered from 36 elements and one compound has been measured over the energy interval 60 kev to 1800 kev. The results are presented in terms of the coefficients of a Legendre-polynomial expansion of the differential scattering cross section in the laboratory coordinate system. All of the data have been corrected for attenuation of the primary beam and a representative part of the data has been corrected for multiple scattering and for the finite angular resolution of the experimental equipment. The analytical details of the multiple (essentially, double) scattering corrections are given in an appendix.

I. INTRODUCTION

INCLUDED in this paper are the results of a survey of the angular distributions of neutrons scattered from 36 elements and one compound, the energy range being 60 to 1800 kev. Measurements were made at intervals of about 80 kev for each element; the energy spread was approximately 100 kev at the lower energies, decreasing to about 60 kev at the higher incident energies. In order to present these data in a practical form, it was decided to represent the differential cross section by an expansion in a series of Legendre polynomials:

$$\sigma_s(\mu)=(\sigma_s/4\pi)\sum_{l=0}^{N-1}\omega_l P_l(\mu), \qquad (1)$$

where μ is the cosine of the scattering angle, σ_s is the integrated scattering (elastic plus inelastic) cross section, and $\sigma_s(\mu)$ is the differential scattering cross section; thus

$$\omega_0=1.$$

By plotting ω_l as a function of the incident neutron energy E_n, it is thus possible to obtain a relatively compact description of the angular distribution for the various atomic numbers, Z, of the scattering elements. Figure 1 is such a plot of σ_s and ω_l ($l=1, \cdots, 4$), referred to the laboratory coordinate system, for the values of Z and E_n measured in this survey. These five graphs, totalling about 170 curves, represent data equivalent to some 800 of the traditional cosine plots. Individual graphs (for given Z) of σ_s and ω_l as functions of E_n are contained in an Argonne Laboratory report.[1]

All of the data have been corrected for the attenuation of the primary beam and a representative portion has been corrected for multiple scattering and for the finite angular resolution of the experimental equipment. The details of these corrections are discussed in Sec. III. A statistical analysis of part of the data, as well as the observation of general consistency, indicated standard deviations of approximately ± 0.05 for ω_1, ± 0.10 for ω_4, and intermediate accuracies for ω_2 and ω_3. These deviations are roughly independent of the values of ω_l. The statistical accuracy of σ_s is better than 10% in most cases.

Measurements of the differential cross sections for elastic scattering have been published[2–4] for some of the neutron energies and scattering samples used in this survey. A comparison of such data with the scattering cross sections should give an indication of the magnitude of the inelastic scattering cross section. These results are summarized in Tables I and II.

In order that the series (1) give a valid extrapolation of $\sigma_s(\mu)$ for angles other than those at which measurements were made, it is necessary that ω_l be negligible for $l \geq N$. Here $N=5$ since the measurements were made at five fixed scattering angles. The small magnitudes of ω_3 and ω_4 as well as the agreement between the extrapolation of Eq. (1) and the measurement of

TABLE I. Values of σ_s, $\sigma_{n'}$, σ_γ, and σ_{tr} in barns at 1 Mev.

Element	σ_s	$\sigma_{n'}$[a]	σ_γ[b]	σ_{tr}[c]	$\sigma_T-\frac{2}{3}\omega_1\sigma_s$
Ti	3.1	0.3	−0.2	2.1	2.4
Fe	2.2	0.1	0.3	2.1	2.0
Co	3.4	0.1	0.1	3.0	3.0
N	2.9	0.1	0.0	2.5	2.4
C	3.2	0.3	0.0	2.8	2.7
Zn	3.5	0.2	0.1	3.3	3.1
Se	5.0	0.7	0.0	3.5	3.6
Zr	6.4	0.2	0.2	4.6	4.8
No	6.8	1.0	−0.3	4.2	4.4
Mo	6.5	0.8	0.3	4.6	4.4
Ag	6.2	1.7	0.2	4.4	4.2
Cd	6.4	0.9	0.5	4.4	4.3
In	6.5	0.3	0.1	4.1	4.0
Sn	6.2	0.1	0.6	4.6	4.4
Te	6.5	0.6	0.0	3.9	4.0
Ta	6.3	1.2	0.9	5.2	5.2
W	6.5	1.8	0.4	5.3	5.0
Au	5.4	1.3	0.2	4.4	4.2
Pb	5.1	0.5	−0.2	4.1	4.0
Bi	5.1	0.3	−0.2	4.1	4.1
Th	6.2	0.9	0.9	5.3	5.3

[a] $\sigma_{n'}=\sigma_s-\sigma_n$; σ_n given in reference 2.
[b] $\sigma_\gamma=\sigma_T-\sigma_s$; σ_T given in reference 2.
[c] σ_{tr} as defined by Eq. (10a) and measured in reference 2.

* Work performed under the auspices of the U. S. Atomic Energy Commission.

[1] Langsdorf, Lane, and Monahan, Argonne National Laboratory Report ANL-5567, June, 1956 (unpublished).

[2] M. Walt and H. H. Barschall, Phys. Rev. **93**, 1062 (1954).
[3] Darden, Haeberli, and Walton, Phys. Rev. **96**, 836 (1954).
[4] Allen, Walton, Perkins, Olson, and Taschek, Phys. Rev. **104**, 73 (1956).

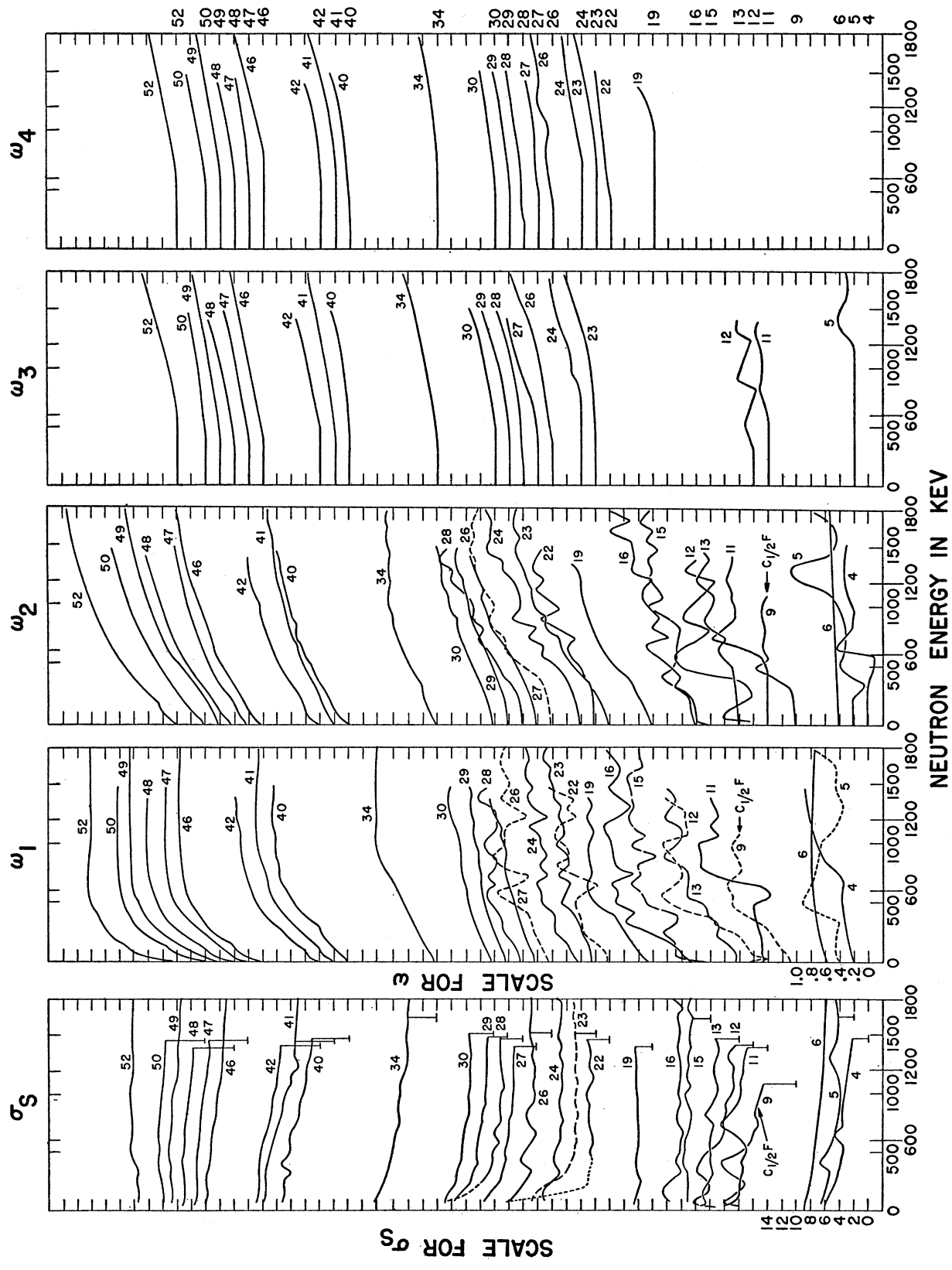
ZERO POSITION FOR VALUE OF Z INDICATED
ω_4
ω_3
ω_2
ω_1
σ_S
SCALE FOR σ_S
SCALE FOR ϵ
NEUTRON ENERGY IN KEV
$C_{1/2}F$

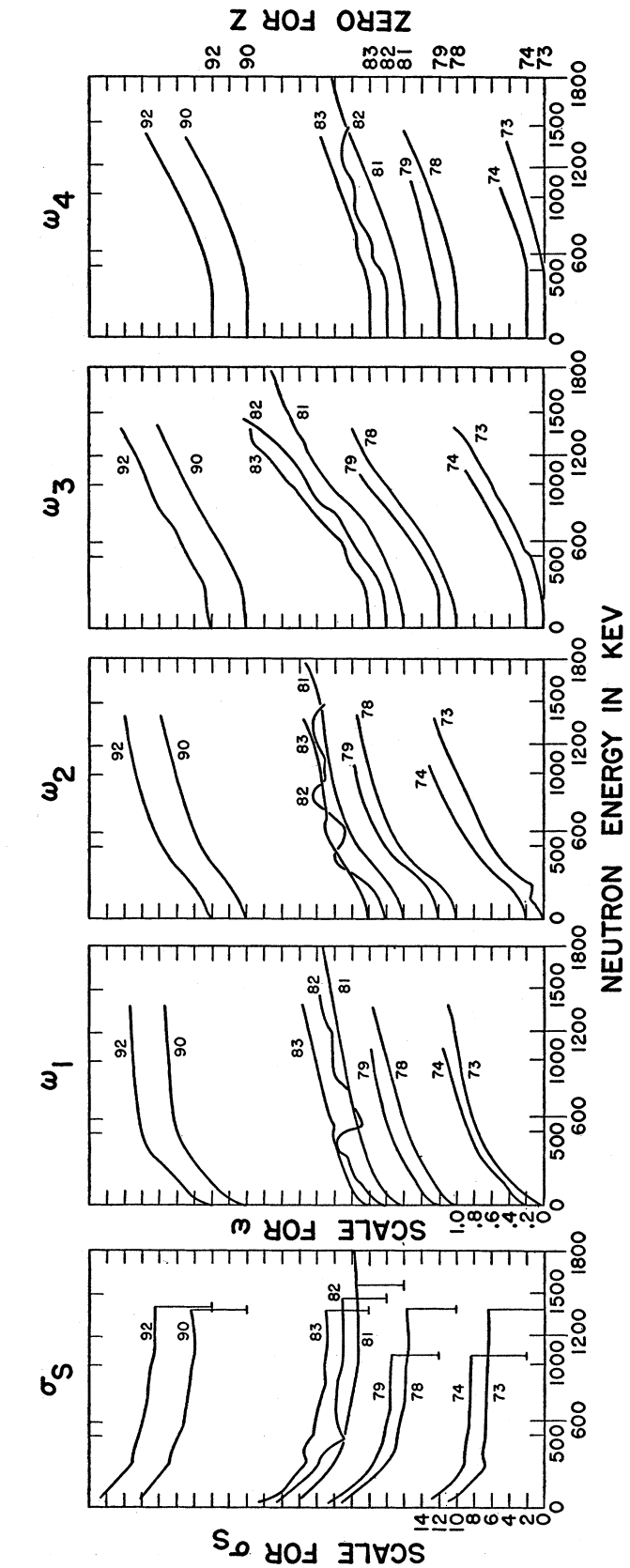

FIG. 1. The differential cross section for scattering of neutrons as a function of Z and E_n in laboratory coordinates and in the representation of Eq. (1), $\sigma_s(\mu)=(\sigma_s/4\pi)\Sigma\omega_l P_l(\mu)$. Data are given for ${}_4$Be, ${}_5$B, ${}_6$C, ${}_{11}$Na, ${}_{12}$Mg, ${}_{13}$Al, ${}_{15}$P, ${}_{16}$S, ${}_{19}$K, ${}_{22}$Ti, ${}_{23}$V, ${}_{24}$Cr, ${}_{26}$Fe, ${}_{27}$Co, ${}_{28}$Ni, ${}_{29}$Cu, ${}_{30}$Zn, ${}_{34}$Se, ${}_{40}$Zr, ${}_{41}$Nb, ${}_{42}$Mo, ${}_{46}$Pd, ${}_{47}$Ag, ${}_{48}$Cd, ${}_{49}$In, ${}_{50}$Sn, ${}_{52}$Te, ${}_{73}$Ta, ${}_{74}$W, ${}_{78}$Pt, ${}_{79}$Au, ${}_{81}$Tl, ${}_{82}$Pb, ${}_{83}$Bi, ${}_{90}$Th, ${}_{92}$U. Data are also given for ${}_9$F, not per atom of F but per "molecule" of C_4F in Teflon. The curves for ω_l are extrapolated to zero energy under the assumption that the angular distributions approach isotropy in the center-of-mass coordinate system as the neutron energy approaches zero. For most materials the lowest energy at which measurements were made is 60 kev; for some there is a point at 30 kev. (Actual experimental points are shown on the curves in reference 1.) For some low-Z elements, curves are not given for ω_3 or ω_4 because, within the accuracy of the data, the value is zero over the entire energy range of the data.

Values of σ_s given here have been compared with published data [D. J. Hughes and J. A. Harvey, *Neutron Cross Sections*, Brookhaven National Laboratory Report BNL-325 (Superintendent of Documents, U. S. Government Printing Office, Washington, D. C., 1955)] on σ_T which are available for all but three elements; agreement is reasonable in most cases. (Usually it is within 10% except when marked differences can be ascribed clearly to the difference in neutron energy spread used.) Data for hydrogen (polyethylene) were also obtained as a check on the method. Since it contributes no information, it has been omitted from this graph. On most of the curves for σ_s, a vertical line attaches the curve to a "foot" bar at the level of the zero for that curve; this was done only as a visual aid in reading the curves.

TABLE II. Values of σ_s, $\sigma_{n'}$, σ_γ, and $\sigma_{el.tr.}$ in barns at 0.5 and 1.0 Mev from a comparison with the measurement reported in reference 4.

Element	E_n	σ_s	$\sigma_{n'}$	σ_γ	$\sigma_{el.tr.}$	$\sigma_n-\frac{2}{3}\omega_1\sigma_s$
Au	0.5	6.3	0.9	0.0	4.0	4.2
Bi	0.5	6.5	0.2	−0.2	5.4	5.4
U	0.5	8.4	1.1	−0.2	4.7	5.1
U	1.0	6.8	1.4	0.1	3.5	3.4

Darden, Haeberlin, and Walton[3] at small scattering angles insure the adequacy of this series with $N=5$ for all but the heaviest elements at energies well above 1 Mev.

II. EXPERIMENTAL

A description of the apparatus used in obtaining these data will be submitted for publication in another journal. This section will be limited, therefore, to a discussion of those aspects of experimental equipment and technique which are peculiar to these measurements.

The primary neutron source was a Li^7 target bombarded by a beam of protons from the Argonne Van de Graaff generator. This source was located in the cavity of a tank filled with borated water. A collimating tube from the cavity to the exterior of the tank permitted a beam of neutrons from the source to impinge on a thin flat plate of scattering material. Five neutron detectors were placed in a circular array around the scatterer so that neutrons were counted simultaneously at five angles. Each neutron detector contained an assembly of ten BF_3 proportional counters immersed in an aluminum tank filled with mineral oil. The aluminum tanks were placed inside a shield consisting of a steel tank containing borated water. A collimator hole permitted neutrons from the scattering sample to reach the counter assembly.

In most neutron scattering apparatus, adequately precise monitoring of the flux incident on the scatterer is very difficult. By measuring five angles at once, monitoring becomes somewhat less important. However, quite satisfactory monitoring was obtained by locating two BF_3 counters close to the collimator tube in the tank assembly which shielded the source. In this geometry, even with very thick scatterers, back-scattering perturbs the monitor a negligible amount (a fraction of a percent for a scatterer with a thickness of more than a mean free path).

The distance from the neutron source to the center of the scatterer was 5 feet; scatterer-to-detector distance, 7 feet; "illuminated" area of the scatterer measured normal to the direction of the incident beam, 6 inches wide by 16 inches high; and the effective detector area, also 6 inches by 16 inches. The water tanks were in the form of truncated pie-shaped wedges which would fit together side by side to form a circular array. At the center of the scatterer, each of these five tanks, which shielded the detectors, subtended an angle of 30° in the horizontal plane and the tank shielding the source subtended an angle of 40°. Thus the water shielding very nearly filled all of the available space. The adequacy of this shielding was tested by plugging the collimator hole of one unit. This reduced the counting rate for 1-Mev neutrons by a factor of more than 2000.

The nominal[5] scattering angles were 22°18′, 54°4′, 91°40′, 112°25′, and 143°54′. For these nominal angles, but taking account of extended size of the scatterers and detectors employed, the mean scattering angles were calculated to be 24°3′, 55°24′, 91°12′, 112°48′, and 143°42′, respectively. The effective angular resolution was approximately 5° for the counters at 26°, 55°, and 91° and approximately 3° for the other counters. These calculations were made for the geometrical conditions of the experiment, including the fact that the scattering samples were mounted vertically with the beam incident at an angle of 45° from the normal to the plate surface. The first three detectors were placed to observe neutrons emerging from the side of the plate opposite that from which the beam was incident (transmission geometry). The last two detectors (those at 113° and 144°) observed neutrons scattered from the reflection side of the scattering plate. The fact that the spread in angle in transmission geometry is twice that in reflection geometry is a characteristic difference between these two cases.

The oblique orientation of the scattering plate with respect to the direction of the incident beam was a practical compromise chosen to minimize the multiple-scattering corrections. It is clear that nearly all neutrons will be multiply scattered away from any direction which is nearly in the plane of the scattering plate. With the orientation chosen, no data were taken at a direction of emergence making an angle greater than 47° from the normal to the surface of the plate. In this way it was possible to limit the magnitude of the perturbations due to multiple scattering so that the calculated corrections to any initial (uncorrected) differential cross section were never over 35%, even in the most extreme cases that have been calculated, and were a good deal less than this in most cases.

Since BF_3 counters in a moderator detect neutrons of all energies, this apparatus measured total scattering rather than elastic scattering. In order that the measured differential cross section be a simple sum of the contributions from elastic and inelastic scattering, it is necessary that the efficiency of the detectors be independent of neutron energy. Various arrays of the ten counters in each assembly were tried until an array was obtained for which the response was uniform with energy to within 10% relative to a "long counter" from 0.10 Mev to 1.50 Mev.

Tests with various neutron sources [photosources of

[5] The nominal scattering angles are defined here as the angle included between the direction of a line from the source to the midpoint of the scatterer and the direction of a line from the midpoint of the scatterer to the midpoint of the detector.

Sb-Be, Na-Be, Na-D_2O, and mixed Ra(α)-Be] showed the five counters to be equally efficient within about 2%. (The data were corrected to uniform efficiency.) The absolute efficiency for counting neutrons incident on the face of each detector was between 15 and 20%. Using a neutron source consisting of a lithium target of 10-kev stopping power, about 300 counts per minute per detector were obtained with a 15-microampere proton beam.

The background counting rate was predominately due to air scattering. Each detector, in addition to the scattering sample, also "saw" a column of air about 2 feet long which was "illuminated" by the primary neutron beam. This amount of air scatters about 1% of the incident neutrons. Thus background counting rates were predicted to be, and indeed were found to be, about 10% of the rate due to a typical scatterer which had a transmission of 90%.

Also studied was the extent of the counting rate which might be attributed to neutrons which, already scattered by the scattering sample, were re-scattered by the air or shielding "visible" to a given detector. This effect was investigated by placing a Na-Be photoneutron source near the usual position of the scatterer and observing the counting rate of a given detector with and without a shadow-cone shield interposed between the source and the detector. In this manner an upper limit of 2%, relative to the direct flux from the source, was placed on the amount of such scattering. Of this, roughly half was produced by air scattering and half by other materials. No corrections for this phenomenon have been made for the data presented in this paper.

III. ANALYSIS OF THE DATA

In brief, the scheme of analysis involves the reduction of the counting information to a representation of the differential cross section in terms of the coefficients of a series of Legendre polynomials. These coefficients are then used to correct the observed counting rates for multiple scattering. Since the correction itself depends on the corrected distribution, this calculation is necessarily carried through by iteration. For most of the data presented here, a single iteration gives this correction well within the statistical accuracy of the experiment. This calculation also takes into account the attenuation of the primary beam and the finite angular resolution of the experimental equipment.

It is convenient to make the following assumptions: (1) Since the energy spread of the incident neutron beam used in obtaining these data was very nearly 100 kev, the quantity measured was very nearly

$$\langle\sigma_s(\mu)\rangle_{\text{Av}}=\int I(E)\sigma_s(\mu,E)dE\Big/\int I(E)dE,$$

where $I(E)$ is the distribution function for the energy spectrum of the primary beam. It is assumed that all effects, such as "beam hardening" and energy loss on scattering, which cause a variation in $I(E)$ can be neglected in the interpretation of $\langle\sigma_s(\mu)\rangle_{\text{Av}}$. In the following the brackets will be omitted in the designation of this cross section. (2) All polarization effects are neglected. (3) Reactions leading to the disappearance of a neutron or to the multiple production of neutrons are negligible compared with neutron scattering. It is convenient to define the following symbols:

Φ_0 is the flux[6] incident on the scattering plate. A is the area of the scatterer "illuminated" by the inciden beam. N^Z is the thickness (in atoms/cm^2) of the scattering sample, measured in the direction of the normal to the plane of the plate. α is the secant of the angle included between the directions of Φ_0 and the normal to the scattering plate. $\sigma_T{}^Z$ is the total neutron cross section of the sample. $\sigma_s{}^Z(\mu)$ is the differential (elastic plus inelastic) scattering cross section, in barns per steradian, of the sample of atomic number Z. ϵ_j is the efficiency of the detector at the scattering angle $\cos^{-1}\mu_j$. $\Delta\Omega_j$ is the solid angle subtended by this detector at the scattering target. $G^Z(\mu_j)$ is the gross number of counts recorded by the jth counter for a scattering element of atomic number Z, normalized to a standard count as measured by a monitor whose count is proportional to the forward-neutron output of the Li(p,n) source. $B(\mu_j)$ is the observed background count normalized to the same standard monitor count as $G^Z(\mu_j)$.

The number of counts recorded by the jth counter due to scattering by the sample Z is given by

$$G^Z(\mu_j)-B(\mu_j)=\epsilon_j\Delta\Omega_jA\Phi_0\sigma_s{}^Z(\mu_j)[\alpha\sigma_T{}^Z]^{-1}\times[1-\exp(-\alpha N^Z\sigma_T{}^Z)].$$

This quantity is measured using the several separate detectors set up at the various scattering angles identified by the index j. These counters have slightly differing values of ϵ_j and $\Delta\Omega_j$. By a separate measurement using a rotating neutron source, as discussed in Sec. II, it is possible to determine a set of correction factors ρ_j such that the product $k=\rho_j\epsilon_j\Delta\Omega_j\alpha^{-1}A\Phi_0$ is the same for all angles measured. The corrected count is then given by

$$\begin{aligned}C^Z(\mu_j)&=\rho_j[G^Z(\mu_j)-B(\mu_j)]\\&=k\sigma_s{}^Z(\mu_j)[\sigma_T{}^Z]^{-1}[1-\exp(-\alpha N^Z\sigma_T{}^Z)],\end{aligned}\quad(2a)$$

where, to a good approximation,[7]

$$\sigma_s{}^Z(\mu_j)=\int_{\Delta\Omega_j}\sigma_s{}^Z(\mu)d\Omega/\Delta\Omega_j.\quad(2b)$$

[6] In this discussion the term "flux" is used to denote the number of neutrons incident on unit area in a specified time.

[7] Equation (2b) would properly be written as a multiple integral over the face of the scatterer, the integration limits $\Delta\Omega_j$ being functions of the position coordinates on the scatterer. Further, the integrand should be weighted by the efficiency of the detector as a function of the integration variables. The integral (2b), or more properly (3b), actually was evaluated using the angular spreads given in Sec. II and treating the detector efficiency as a constant over these angles. Since this procedure, which undoubtedly gives an overestimate, resulted in a correction of the differential cross section of less than 1%, these approximations were considered to be sufficiently accurate.

From (1), one obtains

$$\sigma_s^Z(\mu_j)=(\sigma_s^Z/4\pi)\sum_{l=0}^{N-1}\omega_l\mathcal{P}_{jl},\quad j=1,\cdots,N,\quad (3a)$$

where the elements of the $N\times N$ matrix are defined as

$$\mathcal{P}_{jl}=\int_{\Delta\Omega_j}P_l(\mu)d\Omega/\Delta\Omega_j.\quad (3b)$$

Substituting (3a) into (2a) and solving the resulting equation for ω_l, one obtains

$$\omega_l=4\pi\sigma_T^Z\sum_{j=1}^{N}\mathcal{P}_{lj}^{-1}C^Z(\mu_j)\times\{k\sigma_s^Z[1-\exp(-\alpha N^Z\sigma_T^Z)]\}^{-1},\quad (4a)$$

or, since $\omega_0=1$,

$$\omega_l=\frac{\omega_l}{\omega_0}=\sum_{j=1}^{N}\mathcal{P}_{lj}^{-1}C^Z(\mu_j)/\sum_{j=1}^{N}\mathcal{P}_{0j}^{-1}C^Z(\mu_j),\quad (4b)$$

where $\mathcal{P}_{lj}^{-1}$ denotes the lj-component of the inverse of the matrix $\mathcal{P}$.

Although the coefficients ω_l depend only on the relative efficiency of the counters, it is necessary to evaluate the constant k in order to obtain σ_s^Z. This is done by normalizing all integrated scattering cross sections to the cross section of an independently measured standard. For neutron energies below 2 Mev the best material for this purpose is carbon; it exhibits no inelastic scattering, no resonance structure, and entirely negligible capture. Replacing the symbol Z by C to denote a carbon sample and considering $\sigma_T^C=\sigma_s^C$, as known from independent transmission measurements, one obtains from the $l=0$ equation of the set (4a)

$$k=4\pi\sum_{j=1}^{N}\mathcal{P}_{0j}^{-1}C^C(\mu_j)[1-\exp(-\alpha N^C\sigma_s^C)]^{-1}.\quad (5)$$

For any sample Z, the total cross section can be expressed in terms of the scattering cross section as

$$\sigma_T^Z=(1+\delta)\sigma_s^Z,\quad (6)$$

in which $\delta\geq 0$. Introducing (6) into the $l=0$ equation of (4a) and solving for the scattering cross section, one obtains

$$\sigma_s^Z=-[\alpha N^Z(1+\delta)]^{-1}\times\ln\{1-4\pi k^{-1}(1+\delta)\sum_{j=1}^{N}\mathcal{P}_{0j}^{-1}C^Z(\mu_j)\}.\quad (7)$$

As long as the scattering sample is not too thick, σ_s^Z can be obtained quite accurately by setting δ equal to zero in (7). Only in exceptional cases will δ exceed 0.1 and even then, for the samples used in this experiment, the error introduced in σ_s^Z by this approximation is less than 2%. Hence, in all calculations, we set $\delta=0$.

Thus far the effect of multiple scattering has been neglected in the interpretation of the quantity $C^Z(\mu_j)$ in Eq. (2a). Actually, however, the observed number of counts is given by

$$\rho_j[G^Z(\mu_j)-B(\mu_j)]=k\sum_t\Phi_t(h^Z,\mu_j),$$

where $k\Phi_t(h^Z,\mu_j)$ is the number of neutrons detected by the jth counter after having been scattered t times in the scattering sample characterized by $h^Z=N^Z\sigma_T^Z$. Thus the correct value of $C^Z(\mu_j)$ in (4a) and subsequent equations is

$$\left\{\frac{[1-\exp(-\alpha N^Z\sigma_T^Z)]\sigma_s^Z(\mu_j)}{\sigma_T^Z\sum_t\Phi_t(h^Z,\mu_j)}\right\}\rho_j[G^Z(\mu_j)-B(\mu_j)].\quad (8)$$

Since the bracketed correction factor is itself a function of the angular distribution, these corrections must be carried out by iteration. The details of an exact calculation of $\Phi_1(h^Z,\mu_j)$ and $\Phi_2(h^Z,\mu_j)$ and an approximate calculation of $\sum_{t=3}^{\infty}\Phi_t(h^Z,\mu_j)$ are given in the appendix.

IV. RESULTS

The differential scattering cross section as a function of the atomic number Z of the target element and the incident neutron energy E_n is shown in Fig. 1.

In so far as practical, the notation for the various experimental neutron cross sections which are discussed in this paper conforms to that suggested by Goldstein.[8] The total cross section,[9] σ_T, is the sum of the elastic scattering cross section, σ_n, and the nonelastic cross section σ_X. At the energies of interest in this discussion the only contributions to σ_X which are of importance are the inelastic scattering cross section, $\sigma_{n'}$, and the capture cross section, σ_γ, thus

$$\sigma_T=\sigma_n+\sigma_X=\sigma_n+\sigma_{n'}+\sigma_\gamma=\sigma_s+\sigma_\gamma.\quad (9)$$

The definition of the transport cross section is somewhat variable; however, the most generally accepted one is

$$\sigma_{tr}=\sigma_T-\int\sigma_n(\mu)\mu d\Omega=\sigma_T-\tfrac{1}{3}\omega_1\sigma_s+\int\sigma_{n'}(\mu)\mu d\Omega,\quad (10a)$$

where ω_1 is defined by Eq. (1). For purposes of comparison an elastic transport cross section, $\sigma_{el.tr.}$, is also defined as

$$\sigma_{el.tr.}=\int\sigma_n(\mu)(1-\mu)d\Omega=\sigma_n-\tfrac{1}{3}\omega_1\sigma_s+\int\sigma_{n'}(\mu)\mu d\Omega.\quad (10b)$$

Table I lists the values of $\sigma_{n'}$ and σ_γ obtained by comparing σ_s with the values of σ_n and σ_T at 1 Mev

[8] H. Goldstein, "A Proposed Nomenclature for Experimental Nuclear Cross Sections," May, 1956 (unpublished).

[9] The superscript Z is omitted in this section.

given in reference 2. The fifth column of this table gives the transport cross sections, as defined by (10a), which were measured by Walt and Barschall.[2] The sixth column lists the results of the present measurements, which neglect the last term on the right side of (10a). This is equivalent to assuming that the angular distribution of the inelastically scattered neutrons is isotropic.

Table II summarizes the results of a similar comparison with the measurements of Allen *et al.*[4] at 0.5 Mev and 1.0 Mev.

On the basis of the stated over-all error in the measurement of σ_n and the estimated error in the present measurement of σ_s, the error in $\sigma_{n'}$ is approximately 20% of σ_s while the error in σ_γ is about 15% of σ_s. However, since in both measurements (of σ_n and σ_s) a large part of the error is common to all elements, the relative values of $\sigma_{n'}$ and σ_γ for the various elements are probably considerably more accurate than this.

The transport cross sections measured by Barschall *et al.*[10] at 0.6 Mev and 1.5 Mev are compared with the results of the present experiment in Table III. Our measurements do not include energies of 1.5 Mev for aluminum, cobalt and tungsten.

Figure 2 also is based on the assumption of isotropy for the angular distribution of inelastically scattered neutrons. The solid line represents $\sigma_s(\mu)$ as calculated using Eq. (1) and the coefficients plotted in Fig. 1. The circles and triangles represent $\sigma_n(\mu_j)+\sigma_{n'}/4\pi$, where $\sigma_n(\mu_j)$ is taken from references 2 and 3, respectively, and $\sigma_{n'}$ from Table I. The agreement is seen to be well within the estimated accuracy of the experiments; the same is true for the other elements listed in Tables I and II. However, it is obviously impossible on the basis of this comparison to rule out marked anisotropies in $\sigma_{n'}(\mu)$.

The angular distributions found in the present experiment have been compared[11] with those predicted by the complex-potential model proposed by Feshbach, Porter, and Weisskopf.[12] Both a square-well and a

TABLE III. Comparison with the transport cross sections σ_{tr} in barns measured at 0.6 and 1.5 Mev by Barschall *et al.*[a]

Element	0.6 Mev σ_s	0.6 Mev σ_{tr}	0.6 Mev $\sigma_T-\frac{1}{3}\omega_1\sigma_s$	1.5 Mev σ_s	1.5 Mev σ_{tr}	1.5 Mev $\sigma_T-\frac{1}{3}\omega_1\sigma_s$
Be	4.1	3.4	3.6	2.1	1.4	1.5
C	3.2	2.8	2.8	2.0	1.8	1.8
Al	4.0	3.0	3.0			
Fe	2.6	2.0	2.0	2.9	2.2	2.4
Cu	4.0	3.5	3.5	2.7	2.2	2.2
Co	4.0	3.4	3.5			
W	6.5	4.7	5.0			
Pb	5.7	4.4	5.0	5.0	3.4	3.7

[a] See reference 12.

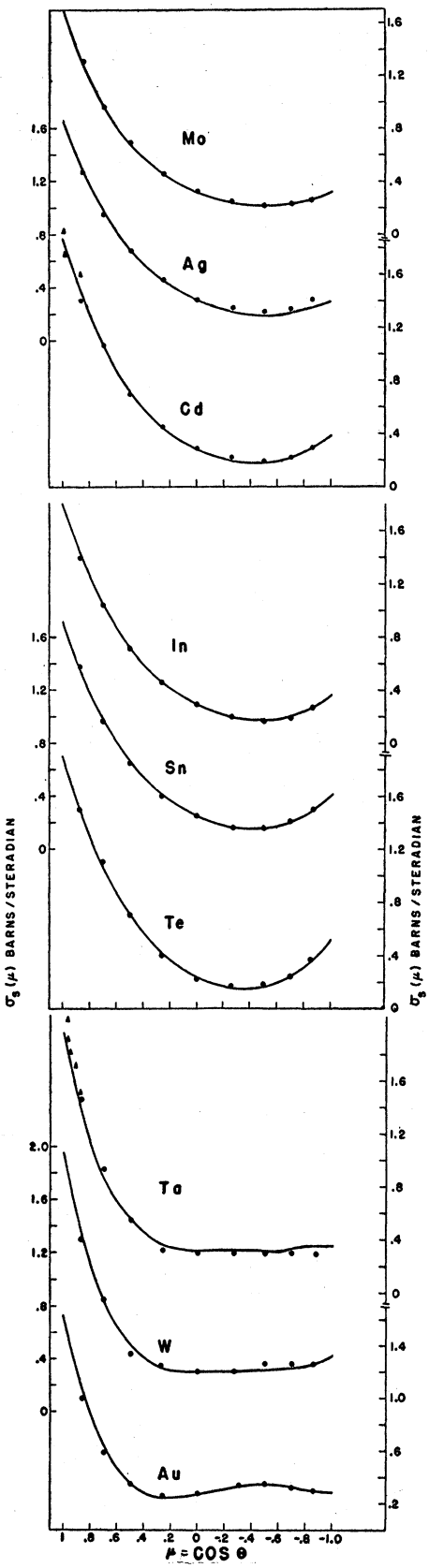

FIG. 2. The differential scattering cross sections of molybdenum, silver, cadmium indium, tin, tellurium, tantalum, and tungsten at 1 Mev. The solid line represents Eq. (1a) evaluated by use of the coefficients determined in the present experiment. The circles and triangles are measurements of $\sigma_n(\mu_j)+\sigma_{n'}/4\pi$, from references 2 and 3.

[10] Barschall, Battat, Bright, Graves, Jorgensen, and Manley, Phys. Rev. **72**, 881 (1947).

[11] Jack Sokoloff, Ph.D. dissertation, Northwestern University, 1956 (unpublished); also Argonne National Laboratory Report ANL-5618 (unpublished).

[12] Feshbach, Porter, and Weisskopf, Phys. Rev. **90**, 166 (1953).

harmonic-oscillator potential were used in an attempt to find a set of parameters by fitting the experimental distributions. In general, the harmonic-oscillator potential results in no better agreement than did the square-well potential. In neither case was it possible to fit the forward peaking nor the peak at approximately 90° in the heavier elements.

V. ACKNOWLEDGMENTS

We wish to thank the staff of the Van de Graaff machine, particularly Jack R. Wallace, William F. Evans, Ronald L. Amrein, and Vincent A. Montelpasse, for their help in the setting-up of the equipment and in performing the experiments. We are also grateful to Donald A. Flanders, Herbert L. Gray, Charles Harrison, and others of the Applied Mathematics Division for their cooperation in the machine computation of these results.

APPENDIX

Although there exists an extensive literature on the subject of multiple scattering, little of it was found to be applicable to the present situation in which a collimated beam of neutrons is incident at an oblique angle on a thin plane-parallel scattering sample which has rather strongly anisotropic scattering properties. Measurements of the type discussed in the caption of Fig. 4 indicated that the effect of multiple scattering on the angular distribution of scattered neutrons was appreciable even for sample thicknesses less than 0.1 mean free path. It was, therefore, necessary to devise a method of correcting for this effect.

The work to be discussed in this appendix results in exact expressions for the emergent single and double scattered flux under the conditions previously described. The assumptions underlying these are those listed in Sec. III. The most important of these assumptions is that the differential cross section is the same for all orders of scattering. Usually this is called the energy-independence assumption. The emergent flux attributable to scattering of order higher than the second is approximated by assuming that the ratio of flux due to successive orders of scattering is independent of the order. Thus, although the assumption of thin plates does not enter formally in these derivations, the use of the method is limited to sample thicknesses for which the contribution of third and higher order processes to the total scattering is not very large.

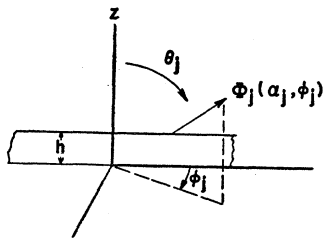

FIG. 3. Geometry of the scattering plate.

Consider a coordinate system oriented with respect to the scatterer as shown in Fig. 3. The thickness of the scatterer, measured along the z direction, is denoted by h. All distances, including h, are measured in units of mean free path. The lateral dimensions of the scattering sample are considered to be essentially infinite compared with h.

The incident flux, whose direction is $(a_0=\alpha_0^{-1}=\cos\theta_0;\ \varphi_0)$ is taken as unity. Thus the flux, $\Phi_l(a_j;\ \varphi_j)$, emergent in the direction $(a_j=\alpha_j^{-1}=\cos\theta_j;\ \varphi_j)$, after having experienced l scatterings is to be interpreted as flux per unit solid angle per unit incident flux. In order to fix the coordinate system uniquely the plane $\varphi_0=0$ is chosen as that defined by the z-axis and the direction of the incident beam, the direction of incidence being chosen so that $a_0>0$.

The scattering sample is characterized by a phase function $p(\mu_{ij})$ defined by

$$p(\mu_{ij})=4\pi\sigma_s(\mu_{ij})/\sigma_T, \tag{A1}$$

where $\sigma_s(\mu_{ij})$ is the differential cross section for scatter ing from the direction (a_i,φ_i) to the direction (a_j,φ_j),

$$\mu_{ij}=a_ia_j+[(1-a_i^2)(1-a_j^2)]^{\frac{1}{2}}\cos(\varphi_i-\varphi_j),$$

and σ_T is the corresponding total cross section. In terms of the expansion coefficients ω_l of Eq. (1), this phase function may be expressed in the form:

$$p(\mu_{ij})=(\sigma_s/\sigma_T)\sum_{l=0}^{N}\omega_l\sum_{m=0}^{l}\frac{(l-m)!}{(l+m)!}(2-\delta_{0m})\times\cos m(\varphi_i-\varphi_j)P_l^m(a_i)P_l^m(a_j), \tag{A2}$$

where $P_l^m(a)$ denote the associated Legendre polynomials as defined in Jahnke-Emde.[13]

The probability of an interaction within an element dz at z resulting in scattering from the direction (a_i,φ_i) into unit solid angle in the direction (a_j,φ_j) is $(4\pi)^{-1}\times|\alpha_i|dzp(\mu_{ij})$. It is convenient to introduce the symbol $\psi_{ij}(z,\mu)$ to denote the product of this and the attenuation $\exp(-|\alpha_i|z)$ between the $(i-1)$st and the ith events; thus

$$\psi_{ij}(z,\mu)dz=(4\pi)^{-1}|\alpha_i|\,p(\mu_{ij})e^{-|\alpha_i|z}dz. \tag{A3}$$

The flux emergent in the (a_1,φ_1)-direction after a single scattering is, for $a_1>0$,

$$\Phi_1(a_1,\varphi_1)=\int_0^h\psi_{01}(z,\mu)e^{-\alpha_1(h-z)}dz=\frac{\alpha_0p(\mu_{01})}{4\pi}\frac{e^{-\alpha_0h}-e^{-\alpha_1h}}{\alpha_1-\alpha_0}, \tag{A4t}$$

since the flux scattered at coordinate z is further attenuated by an amount $\exp[-\alpha_1(h-z)]$ before emerging

[13] E. Jahnke and F. Emde, *Tables of Functions* (Dover Publications, New York, 1945), p. 110.

from the plate. For reflection, the additional attenuation is $e^{\alpha_1 z}$, so that for $a_1<0$

$$\Phi_1(a_1,\varphi_1)=\int_0^h \psi_{01}(z,\mu)e^{\alpha_1 z}dz = \frac{\alpha_0 p(\mu_{01})}{4\pi}\frac{e^{(\alpha_1-\alpha_0)h}-1}{\alpha_1-\alpha_0}. \quad \text{(A4r)}$$

The total emergent single-scattered flux is given by the relation:

$$\Phi_1=\int_0^{2\pi} d\varphi_1\int_{-1}^{1} da_1\Phi_1(a_1,\varphi_1) = (\alpha_0\sigma_s/2\sigma_T)\sum_l \omega_l P_l(a_0)\sum_{j=0}^{l} q_{lj} \times\{e^{-\alpha_0 h}F_{j+2}(h,\alpha_0)+(-1)^j F_{j+2}(h,-\alpha_0)\}, \quad \text{(A5a)}$$

where[14]

$$F_j(\tau,\alpha)=\int_1^\infty \frac{d\beta}{\beta^j(\beta-\alpha)}[1-e^{-\tau(\beta-\alpha)}] = \int_0^\tau dt e^{\alpha t}\int_1^\infty \frac{d\beta}{\beta^j}e^{-\beta t} \quad \text{(A5b)}$$

and

$$q_{lj}=\begin{cases}(l+j)!(-1)^{(l-j)/2}\left[2^l j!\left(\frac{l+j}{2}\right)!\left(\frac{l-j}{2}\right)!\right]^{-1} & \text{for } (l-j) \text{ even},\\ 0 & \text{for } (l-j) \text{ odd}.\end{cases} \quad \text{(A5c)}$$

To obtain the emergent double-scattered flux, let the first scattering occur in an element dz' at z', the second in dz at z. The product $\psi_{01}(z',\mu)\psi_{12}(|z-z'|,\mu)$ gives the fraction of the incident flux which is first scattered in unit solid angle in the direction (a_1,φ_1) at z' and then rescattered at z into unit solid angle in the direction (a_2,φ_2). Before emerging from the plate the flux is further attenuated by an amount $\exp[-\alpha_2(h-z)]$ for transmission, and by $e^{\alpha_2 z}$ for reflection. Thus, for $a_2>0$,

$$\Phi_2(a_2,\varphi_2)=\int_0^{2\pi} d\varphi_1\int_0^h dz e^{-\alpha_2(h-z)}I = (\sigma_s/\sigma_T)^2\sum_{k=0}^{N}\sum_{l=k}^{N}\omega_l\omega_k Q_{lk}^{(t)}(a_0;a_2,\varphi_2), \quad \text{(A6t)}$$

and for $a_2<0$,

$$\Phi_2(a_2,\varphi_2)=\int_0^{2\pi} d\varphi_1\int_0^h dz e^{\alpha_2 z}I = (\sigma_s/\sigma_T)^2\sum_{k=0}^{N}\sum_{l=k}^{N}\omega_l\omega_k Q_{lk}^{(r)}(a_0;a_2,\varphi_2), \quad \text{(A6r)}$$

where

$$I=\int_0^z dz'\int_0^1 da_1\psi_{01}(z',\mu)\psi_{12}(z-z',\mu) + \int_z^h dz'\int_{-1}^0 da_1\psi_{01}(z',\mu)\psi_{12}(z-z',\mu).$$

The coefficients Q_{lk} can be expressed in terms of the functions defined by Eq. (A5b) as follows: The integration over the variable φ_1 is carried out using Eq. (2) for both of the phase functions in the integrand. The integration over a_1 is made possible by defining the coefficients $g^n{}_{l,k;j}$ by means by the relation[15]

$$P_l{}^n(a)P_k{}^n(a)=\frac{(k+n)!(l+n)!}{(k-n)!(l-n)!}\sum_{i=0}^{l+k} g^n{}_{j,k;j}a^j. \quad \text{(A7)}$$

The resulting integrals involving the variable z' are of the form of Eq. (A5b) so that the final integration over z involves integrals of the form[16]:

$$\mathfrak{F}_j(h,\rho,\alpha)=\int_0^h dz e^{\rho z}F_j(z,\alpha) =\rho^{-1}\{e^{\rho h}F_j(h,\alpha)-F_j(h,\rho+\alpha)\}. \quad \text{(A8)}$$

This procedure gives

$$Q_{l,k}{}^{(t,r)}(a_0;a_2,\varphi_2)=(\alpha_0/8\pi)\sum_{n=0}^{k}(2-\delta_{0n}) \times\cos n\varphi_2 P_{k,l}{}^n(a_0,a_2)\sum_{j=0}^{l+k} g_{l,k;j}{}^n G_j{}^{(t,r)}, \quad \text{(A9a)}$$

where

$$G_j{}^{(t)}=e^{-\alpha_0 h}[\mathfrak{F}_{j+1}(h,\alpha_0-\alpha_2,\alpha_2) +(-1)^j\mathfrak{F}_{j+1}(h,\alpha_0-\alpha_2,-\alpha_0)], \quad \text{(A9b)}$$

$$G_j{}^{(r)}=[\mathfrak{F}_{j+1}(h,-\alpha_0+\alpha_2,\alpha_0) +(-1)^j\mathfrak{F}_{j+1}(h,-\alpha_0+\alpha_2,-\alpha_2)], \quad \text{(A9c)}$$

and

$$P_{l,k}{}^n(a_0,a_2)=(1-\tfrac{1}{2}\delta_{lk}) \times[P_k{}^n(a_0)P_l{}^n(a_2)+P_l{}^n(a_0)P_k{}^n(a_2)]. \quad \text{(A9d)}$$

The integration of $\Phi_2(a_2,\varphi_2)$ over the angular variables to obtain the total emergent double-scattered flux is carried out in reference 1. However, the resulting expression is too unwieldy for practical use and, fortunately, is not necessary for the purpose set forth in this appendix.

[14] The functions $F_j(\tau,\alpha)$ are discussed by S. Chandrasekhar, *Radiative Transfer* (Clarendon Press, Oxford, 1950), p. 375, and are tabulated in the Astrophys. J. **108**, 92 (1948). See also S. Chandrasekhar, Astrophys. J. **109**, 555 (1949).

[15] A table of the coefficients $g^n{}_{l,k;j}$ for $l\leq 4$ is given in reference 1.

[16] Actual evaluation of the functions $\mathfrak{F}_j(h,\rho,\alpha)$ in the cases required here involves values of ρ so small that the use of the solution by integration by parts in Eq. (A8) sometimes requires values of $F_j(h,\alpha)$ accurate to eight significant figures. The tables in reference 14 are hence inadequate. Values of $F_j(h,\alpha)$ were computed to eight figures by a digital computing machine.

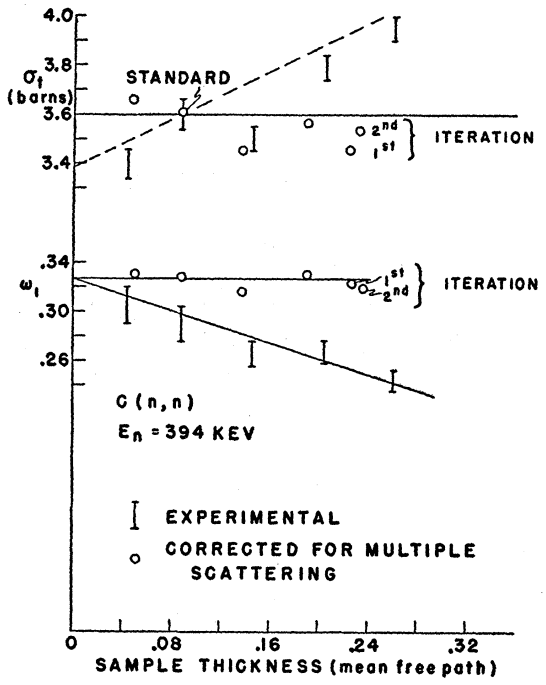

FIG. 4(a)

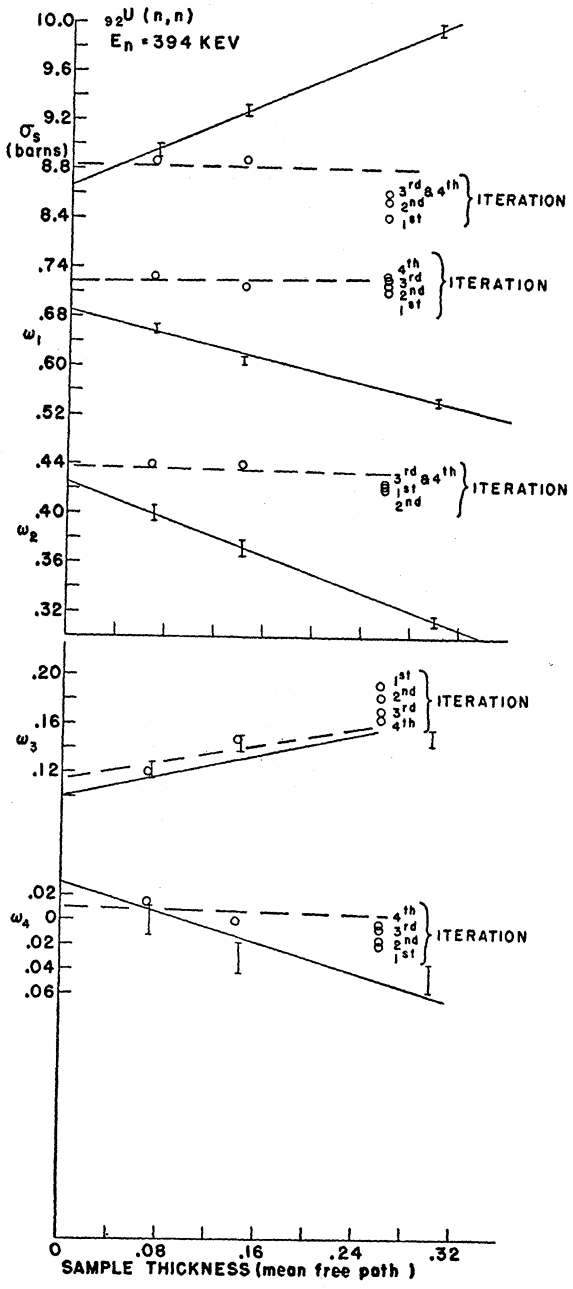

FIG. 4(b)

FIG. 4. (a). The effect of sample thickness upon the calculated parameters for the scattering of 394-kev neutrons by carbon. The vertical bars (which indicate statistical accuracy) are points computed from the experimental data without plural scattering corrections. The scale for σ_s was normalized at the sample for which $h=0.093$ by using as input data the value 3.62 barns for the total cross section of carbon. The open circles indicate the parameters calculated after correction for plural scattering. For the thickest sample the corrections were iterated as shown. (b). The same as Fig. 4(a), except for uranium at 394 kev, again standardized against the carbon sample for which $h=0.093$.

In order to evaluate the correction factor in Eq. (8), the approximation

$$\sum_t \Phi_t(a_0; a_j, \varphi_j) \approx \Phi_1(a_0; a_j, \varphi_j) + \eta \Phi_2(a_0; a_j, \varphi_j) \quad \text{(A10)}$$

is used for the sum over all scattering orders. This approximation is valid provided either that for $t>2$, Φ_t is negligible compared with $\Phi_1+\Phi_2$, or that the angular distribution of the emergent flux which has experienced more than two scatterings is approximately the same as the distribution $\Phi_2(a_0; a_j, \varphi_j)$. The integral of Eq. (A10), together with the assumption[17] that the ratio of successive orders of Φ_t is independent of t, gives

$$\eta \approx (1-e^{-a_0 h})/\Phi_1. \quad \text{(A11)}$$

In the application of these corrections to the angular distribution data, the factor (σ_s/σ_T) in Eqs. (A4) and (A6) was taken as unity.

In order to determine the consistency achieved after

[17] George H. Vineyard, Phys. Rev. 96, 93 (1954), shows that the ratio Φ_{t+1}/Φ_t is approximately independent of t for "quasi-isotropic" scattering.

correcting the data by this method, a few materials were measured with a series of sample thicknesses. The results of these calculations for carbon and uranium are shown in Fig. 4, with detailed explanation in the figure captions.

It is of interest to point out that the functions Q_k are very rapidly varying functions of h, varying about as h^n, $2<n<3$. As a result, $\Phi_2(a_2,\varphi_2)$ is far more sensitive to the value of h, and therefore to σ_T, than to the values of ω_l. Consequently, it was found that most often iteration was necessary almost exclusively in order to obtain a suitably corrected σ_T. Therefore if σ_T is measured independently, accurate results could be obtained with fewer iterations.

PHYSICAL REVIEW VOLUME 107, NUMBER 4 AUGUST 15, 1957

Spontaneous-Fission Half-Lives of Cf^{254} and Cm^{250}†

J. R. HUIZENGA AND H. DIAMOND
Argonne National Laboratory, Lemont, Illinois
(Received May 3, 1957)

Least-squares analysis of spontaneous-fission data obtained over the last four years from a californium sample produced in the November, 1952 thermonuclear test gives a Cf^{254} spontaneous-fission half-life of 56.2 ± 0.7 days in agreement with the astrophysical value of 55 ± 1 days. Some comments are made on the neutron buildup in Type I supernovae and the influence of a possible double magic number, $N=184$, $Z=82$, at $A=266$ on the yield curve near $A=254$. An approximate spontaneous-fission half-life of 2×10^4 years for Cm^{250} is deduced from a curium sample also produced in the November, 1952 thermonuclear test.

CALIFORNIUM-254

A SUGGESTION[1,2] has recently been made that the exponential decay of the light curves ($t_{\frac{1}{2}}=55\pm1$ days) of Type I supernovae is due to the spontaneous-fission decay of Cf^{254}. In the interval 100 days to 640 days after maximum, the light curve of the supernova in *IC* 4182 shows no deviation from an exponential decline.[1] If the above light curve represents the spontaneous-fission decay of Cf^{254}, the astrophysical half-life of Cf^{254} is more precise than the reported half-life values of 60 ± 10 days,[3] 85 ± 15 days,[4] and 55 days[5] determined by spontaneous-fission counting. The first two values were obtained by following the decay of a chemically separated californium fraction containing Cf^{254} produced by the following reactions:

$$\begin{array}{ccc} & & Fm^{254} \\ & & \uparrow \beta^- \\ E^{253}(n,\gamma)E^{254m} & & \sigma=240 \text{ barns.}^6 \\ & & \downarrow \text{E.C.} \\ & & Cf^{254} \end{array}$$

The electron capture to β^- decay ratio of E^{254m} is small, $\sim10^{-3}$, and as a result only very low activities of Cf^{254} have been produced to date by this method.

The other value (55 days) of the Cf^{254} half-life was measured by following a californium fraction[7] separated from the debris of the November, 1952 thermonuclear test ("Mike").

Since the laboratory measurements of the Cf^{254} half-life are in such poor agreement and the recent interpretation of the light curves of Type I supernovae depends on the Cf^{254} half-life being close to 55 days (±1 day),[1] we have analyzed our thermonuclear test data by the least-squares method.

Californium isotopes of mass number 249, 251, 252, 253, and 254 were produced in the test by the reaction paths illustrated in Fig. 1 and were present initially in the sample which has been periodically counted for its spontaneous-fission activity over the last four years. The more recent measurements indicate that the residual activity is decaying with the known half-life of Cf^{252} ($t_{\frac{1}{2}}=2.2\pm0.2$ years; spontaneous-fission half-life of 66 ± 10 years).[8] The spontaneous-fission activity on November 15, 1956 was 0.043 ± 0.001 counts/min which,

† Based on work performed under the auspices of the U. S. Atomic Energy Commission.

[1] Baade, Burbidge, Hoyle, Burbidge, Christy, and Fowler, Astron. Soc. Pacific **68**, 296 (1956).

[2] Burbidge, Hoyle, Burbidge, Christy, and Fowler, Phys. Rev. **103**, 1145 (1956).

[3] Bentley, Diamond, Fields, Friedman, Gindler, Hess, Huizenga, Inghram, Jaffey, Magnusson, Manning, Mech, Pyle, Sjoblom, Stevens, and Studier, *Proceedings of the International Conference on the Peaceful Uses of Atomic Energy, Geneva, August 8–20, 1955* (United Nations, New York, 1956), Vol. 7, p. 261.

[4] Harvey, Thompson, Choppin, and Ghiorso, Phys. Rev. **99**, 337 (1955); A. Ghiorso, *Proceedings of the International Conference on the Peaceful Uses of Atomic Energy, Geneva, August 8–20, 1955* (United Nations, New York, 1956), Vol. 7, p. 15.

[5] Fields, Studier, Diamond, Mech, Inghram, Pyle, Stevens, Fried, Manning, Ghiorso, Thompson, Higgins, and Seaborg, Phys. Rev. **102**, 180 (1956).

[6] Fields, Studier, Mech, Diamond, Friedman, Magnusson, and Huizenga, Phys. Rev. **94**, 209 (1954).

[7] A sample from which the californium and curium fractions were separated was supplied by the Los Alamos Scientific Laboratory.

[8] Magnusson, Studier, Fields, Stevens, Mech, Friedman, Diamond, and Huizenga, Phys. Rev. **96**, 1576 (1954).